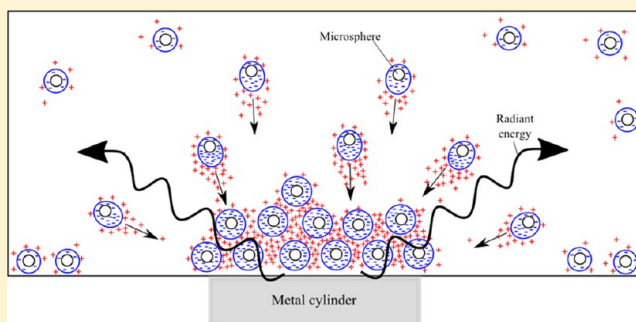


Particle Displacement in Aqueous Suspension Arising from Incident Radiant Energy

Kevin W. Kimura* and Gerald H. Pollack

Department of Chemical Engineering, Department of Bioengineering, University of Washington, Seattle, Washington 98195, United States

ABSTRACT: Colloidal particles in aqueous suspension generally sediment uniformly. By contrast, we found that suspensions of latex microspheres in polystyrene Petri dishes deviated sharply from the expected pattern when various objects were positioned immediately outside those dishes. When small coin-like metal discs were positioned immediately beneath the Petri dish, the microspheres sedimented to a point just above those discs. Other materials, including glass and wood, produced similar results, though less pronounced. After the microspheres had sedimented, shifting the metal to another position beneath the dish caused the microspheres to follow. Various control experiments ruled out trivial explanations. In concordance with earlier results, it appears that the infrared energy generated by the various materials draws microspheres, resulting in the unusual sedimentation patterns. The results have significant implications for the mechanism of sedimentation, particularly for the role of charge in that process.



INTRODUCTION

Aqueous colloidal suspensions are of vital importance because of their ubiquitous presence throughout nature.¹ Colloid sedimentation is thus a heavily researched subject.^{2,3} Understanding sedimentation is of interest in diverse realms, including wastewater treatment, industrial settings, environmental protection, and biological organisms.⁴ Sedimentation is also used to characterize colloids, as embodied in techniques such as field-flow fractionation.^{5,6} Modeling has helped to achieve further understanding of this phenomenon.⁷

Extensive research notwithstanding, numerous properties of colloids and water remain under investigation. This includes the interfacial zone surrounding each suspended colloidal particle and, in particular, the influence of radiant energy on the interfacial zones.⁸

Recent work sheds fresh light on both colloidal dynamics and the role of the interfacial water that surrounds each colloidal particle. Layers of interfacial water, called “exclusion zones” or “EZs” because of their profound exclusionary nature, build next to hydrophilic surfaces. Interfaces of microspheres in aqueous suspension have also been shown to develop EZs. Hence, these interfacial zones may influence colloidal dynamics, including aggregation and sedimentation.

While investigating the impact of variables such as light and charge on microsphere interactions, we came upon an unexpected phenomenon: attraction of suspended microspheres to objects placed outside the chamber. Instead of settling uniformly over the bottom of the chamber, the microspheres accumulated directly over various objects placed immediately beneath. Experiments were performed to explore this phenomenon and deduce its origin.

MATERIALS AND METHODS

The main material used in this experiment was a dilute suspension of carboxylate microspheres (Polysciences, Inc., Polybead carboxylate microspheres, 1 μm , 08226-15). Five drops of microsphere concentrate were added to 50 mL of deionized water, obtained from a Barnstead NANOpure Diamond filter. This produced a concentration of $\sim 1.14 \times 10^7$ particles/L. Five milliliters of this suspension was placed in a Fisherbrand polystyrene Petri dish (50 mm diameter \times 15 mm height) and covered with a plastic lid. Use of the lid was important for minimizing the disruptive effects of evaporation and ambient air currents. By approximately 24 h, the microspheres uniformly settle to the bottom of the Petri dish, covering the entire floor, as shown in Figure 1.

All pictures were taken with a Kodak EasyShare P880 on the “close-image” setting, 20 cm from the Petri dish under the ambient light. For obtaining IR images, we used an uncooled VOx microbolometer (spectral response: 7.5–14 μm ; sensitivity: < 60 mK @ f/1.0). For charging surfaces, a Zerostat 3 Antistatic Gun charge gun was used along with a CharlesWater EMIT 50597 Digital Static Field Meter to measure the surface charge.

Materials used for the experiments included the following: ultramachinable brass (alloy 360); unpolished multipurpose 6061 aluminum; multipurpose 304 stainless steel; multipurpose copper (alloy 110); and glass slides (width and length: 2 cm; height: 5.75 mm). All metals were lathed into cylindrical pellets (diameter: 9.5 mm; height: 5.75 mm). Aluminum samples were also milled into blocks (width and length: 2 cm; height: 1 cm). In some experiments we used a 5 mW laser diode (wavelength 650 nm). All experiments were

Received: June 3, 2015

Revised: September 1, 2015

Published: September 3, 2015

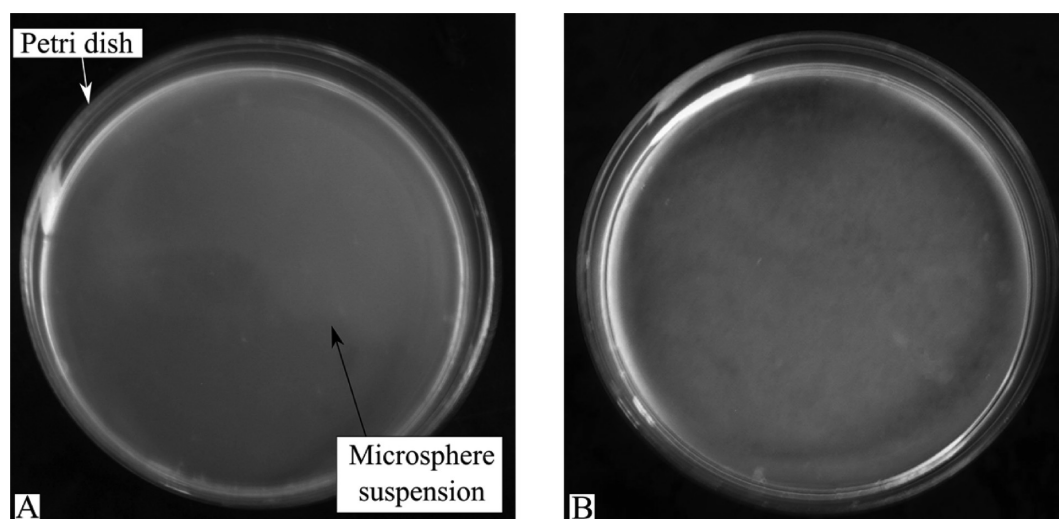


Figure 1. Control experiment. (A) Initial microsphere suspension. (B) Sedimented microspheres after 24 h. Lid was removed immediately prior to taking these pictures. Microspheres sediment moderately uniformly in the center.

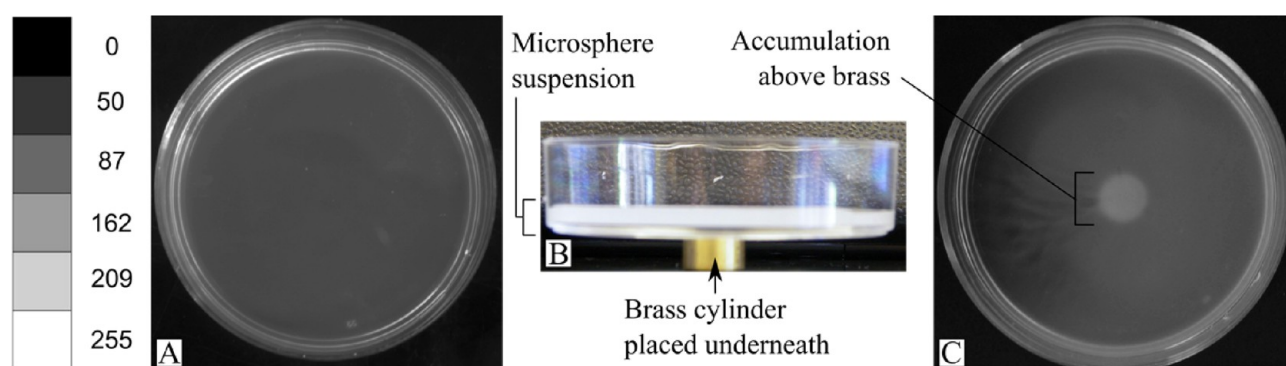


Figure 2. (A) Initial microsphere suspension. (B) Side view of setup before sedimentation began. The Petri dish was filled to approximately one-third of its height. (C) Microspheres settled after 24 h. Left: Grayscale of images.

conducted on top of a black epoxy resin lab bench. Laboratory temperature was thermostatically maintained at 20–21 °C.

RESULTS

Figure 2 shows the results obtained 24 h after a Petri dish was filled with 5 mL of microsphere suspension where a brass cylindrical pellet had been placed directly beneath. A bubble level (Hokins 09815 BullsEye Level) confirmed that the Petri dish was in the horizontal plane. The microspheres sedimented just above the brass piece.

Variants of this experiment were pursued. Figure 3A,B shows the respective accumulations for copper and aluminum. Accumulations were similar to brass. Steel and stainless steel (not shown) also resulted in strongly localized accumulations. Although nonmetal materials were not the focus of this investigation, Figure 3C–F show the results obtained using various other materials. In the case of water beneath (Figure 3C), the Pyrex glass container was filled to the brim with deionized water and placed beneath the Petri dish. Both the water and rim of the glass container touched the bottom of the Petri dish. The result was a strong accumulation of microspheres directly above the water, and a microsphere void directly above the rim of the container. The squared pieces of nonmetal materials, including glass (Figure 3D), pine wood (Figure 3E), and extruded polystyrene foam (not shown) yielded significantly lower accumulations. Polystyrene slides

made from the same material as the Petri dishes showed no discernible accumulation (Figure 3F). Overall, metals produced the strongest accumulations.

To test whether the results might have arisen from the particular type of microsphere used, we tested microspheres with different surface groups, including polystyrene, aldehyde, amine, and amino. Similar results were found. Changing the microsphere dilution over the range of 1 drop per 50 mL to 10 drops per 50 mL did not affect the phenomenon notably; however, 5 drops per 50 mL dilutions were found to be optimal for visual detection. Increasing the volume of microsphere suspension from a range of 5 to 20 mL did not make a difference, even when the Petri dish was completely filled with no air pockets. Volumes larger than 5 mL did require more than 24 h for full sedimentation. Using multiple metal discs and varying the locations of those discs beneath the Petri dish still yielded microsphere accumulations directly above the discs. When the assembly was enclosed within a light-tight, thermally insulated box, similar accumulations persisted.

Visual observation showed all of the metals (stainless steel, brass, copper, aluminum, and steel) producing equally distinct accumulations after 24 h. However, quantitative analysis showed some differences. A densitometric analysis made 10 h into the 24-h period indicated that brass and aluminum produced a relatively higher rate of accumulation, as shown in Figure 4. ImageJ was used to determine the intensity averaged

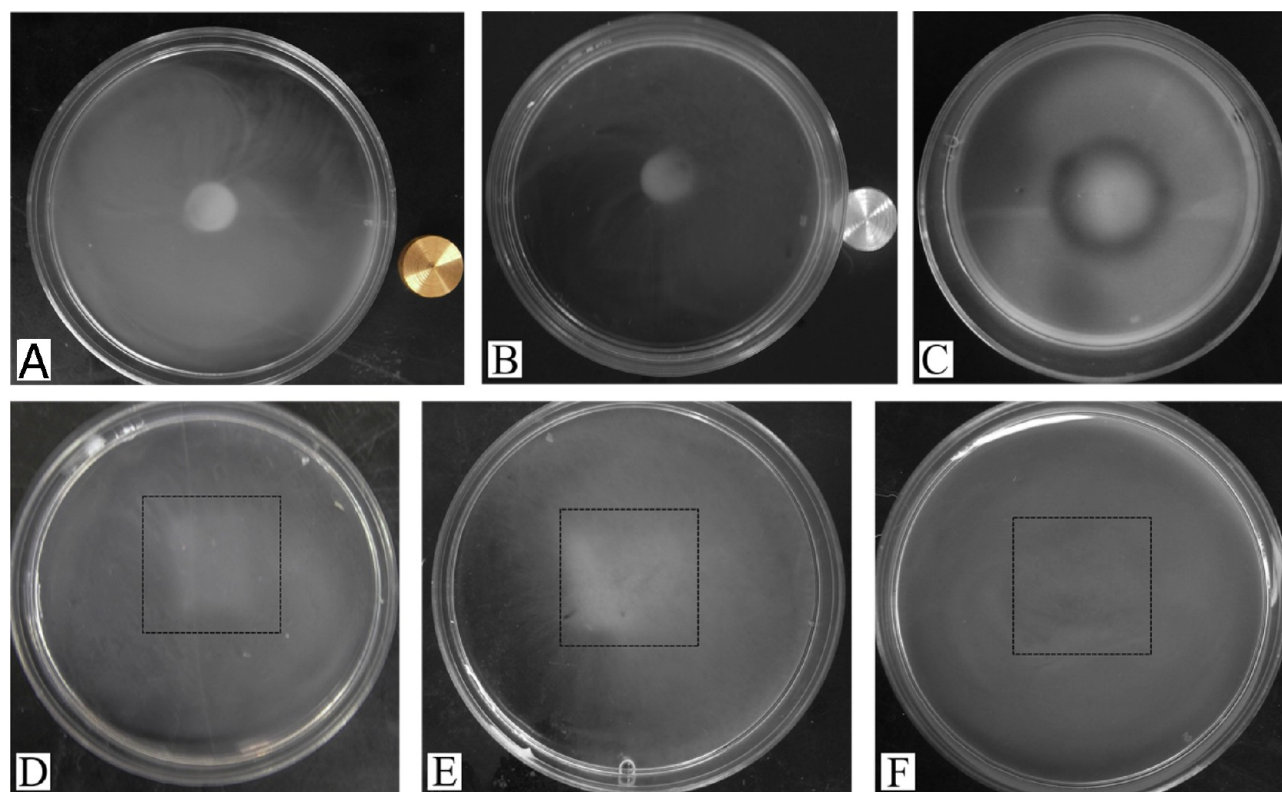


Figure 3. Microspheres sedimented after 24 h, for (A) copper, (B) aluminum, (C) glass bottle filled with DI water, (D) 2 cm x 2 cm glass slide, (E) 2 cm x 2 cm wood (pine), and (F) 2 cm x 2 cm polystyrene. Note: Panels A and B show the metallic pieces set to the side after the experiment, for clear visualization. Drawn rectangles in panels D-F indicate size of material beneath. See Figure 8 for a picture of materials used.

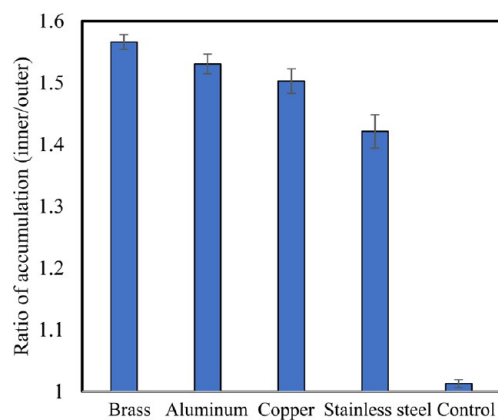


Figure 4. Pixel intensity ratio of inner accumulation circle to outer bulk, measured after a 10-h period. $n_{\text{brass}} = 6$, $n_{\text{Al}} = 4$, $n_{\text{copper}} = 4$, $n_{\text{stainless steel}} = 3$, brass versus stainless steel $p < 0.02$, stainless steel versus control $p < 0.002$.

over the circle of accumulation relative to the outer bulk. Accumulation was highest over the brass, less over the aluminum, still less over the copper, and lowest over stainless steel. Although the differences were small, brass and aluminum seem to exert relatively stronger attraction of the microspheres than copper and stainless steel. Qualitatively, brass and aluminum tended to create sharp, distinct edges around the circle of accumulation; whereas, copper and stainless steel often produced slightly blurred edges.

Post-Sedimentation Movement. We investigated whether microspheres were capable of movement after they had settled. Figure 5 shows that previously settled microspheres

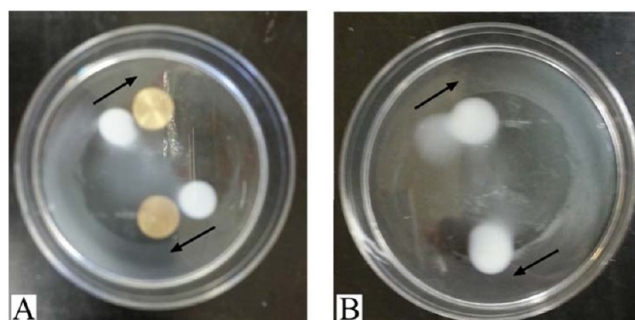


Figure 5. (A) Microspheres accumulated after 24 h with two brass pieces under the Petri dish. Brass pieces were then shifted to positions indicated by arrows. (B) New accumulations 24 h following the metal shift.

easily relocated to positions just above the new location of the metals. This confirms that some attractive force pulls the microspheres toward the metal.

Laser Diode Experiments. Figure 6 shows the results obtained when an aluminum block (width, length: 2 cm; height: 1 cm) was placed under the Petri dish containing the microsphere suspension. In Figure 6A no light was added. In Figure 6B the light output from a red laser diode was directed to the side of the aluminum block for 24 h resulting in increased accumulation. Measurements made using a 1 mm thermocouple (Omega HH306A) showed that the laser-illuminated aluminum had the same temperature as the unilluminated aluminum, within ± 0.1 °C.

Aluminum on Top of Lid. Figure 7 shows the effects of placing an aluminum pellet above the Petri dish lid rather than

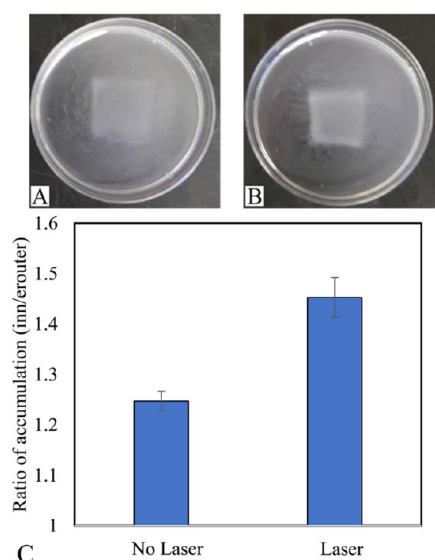


Figure 6. (A) Accumulation after 24 h with aluminum block placed under Petri dish. (B) Same aluminum block illuminated from the side with laser light. (C) Ratio of pixel intensity averaged within square to pixel intensity averaged outside square. $n_{\text{no laser}} = 4$; $n_{\text{laser}} = 4$; $p < 0.002$.

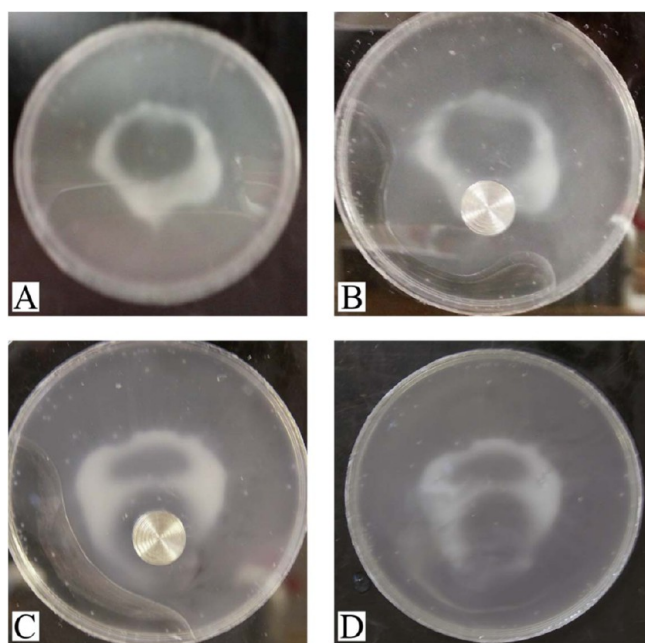


Figure 7. (A) Sedimentation pattern after 24 h with aluminum placed on top of Petri dish lid near the center. (B) Taken immediately after A, showing the pellet just shifted to new location. (C) Result after another 24 h. (D) Taken immediately after C but with lid and aluminum piece removed for clarity.

beneath the Petri dish. The amount of aqueous microsphere suspension in the Petri dish was large enough (~20 mL) to contact the lid above. After 24 h, the microspheres accumulated in the middle of the dish, but with a distinct absence of microspheres directly underneath the metal pellet (Figure 7A). The metal pellet was then shifted to a new location (Figure 7B). Another 24 h later the microspheres had again shifted away from the aluminum (Figure 7C,D).

Figure 8 shows the visible and infrared (IR) light emitted from the various materials used in this study. Among the

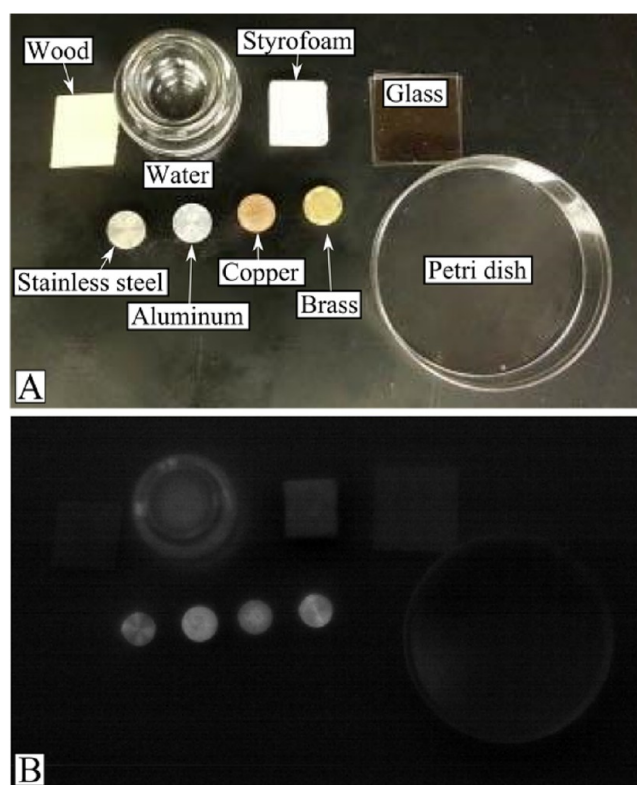


Figure 8. (A) Optical image of the various materials used in this study. (B) Infrared image (7–14 μm emission band) of the same materials.

metals, the highest to lowest IR emissions are as follows: brass, aluminum, stainless steel, and copper. Additionally, the deionized water sample is brighter than the background, while the rim of the surrounding glass jar is considerably darker than the water. (The bright ring around the dark rim comes from the radiant energy emerging from the water outside the rim of the bottle). The glass, wood, and Styrofoam are only slightly brighter than the background. The trend of relative IR emission from the various materials shows a rough correlation with the relative attractive forces, i.e., high IR emission tends to correlate with greater accumulation.

DISCUSSION

The results demonstrate that particles suspended in water are attracted to a variety of different materials. When microspheres are allowed to sediment out of the water, they accumulated just above each of the various materials placed immediately beneath the chamber. Even after settling, the microspheres are attracted toward newly shifted material.

Of the materials studied, we found that metals produced the highest attractive force. Among metals, the rate of accumulation increased in the following order: stainless steel, copper, aluminum, and brass. Exposing the metal to laser light increased the accumulation rate, and placing the metal above the Petri dish caused a circular void to appear beneath the metal, with microspheres forming a ring around the void.

The attraction of microspheres toward materials is unexpected because no obvious attractive mechanism exists. We considered several possible hypotheses to explain the results.

Magnetic Force Hypothesis. Could some kind of magnetic force bear responsibility for drawing the micro-

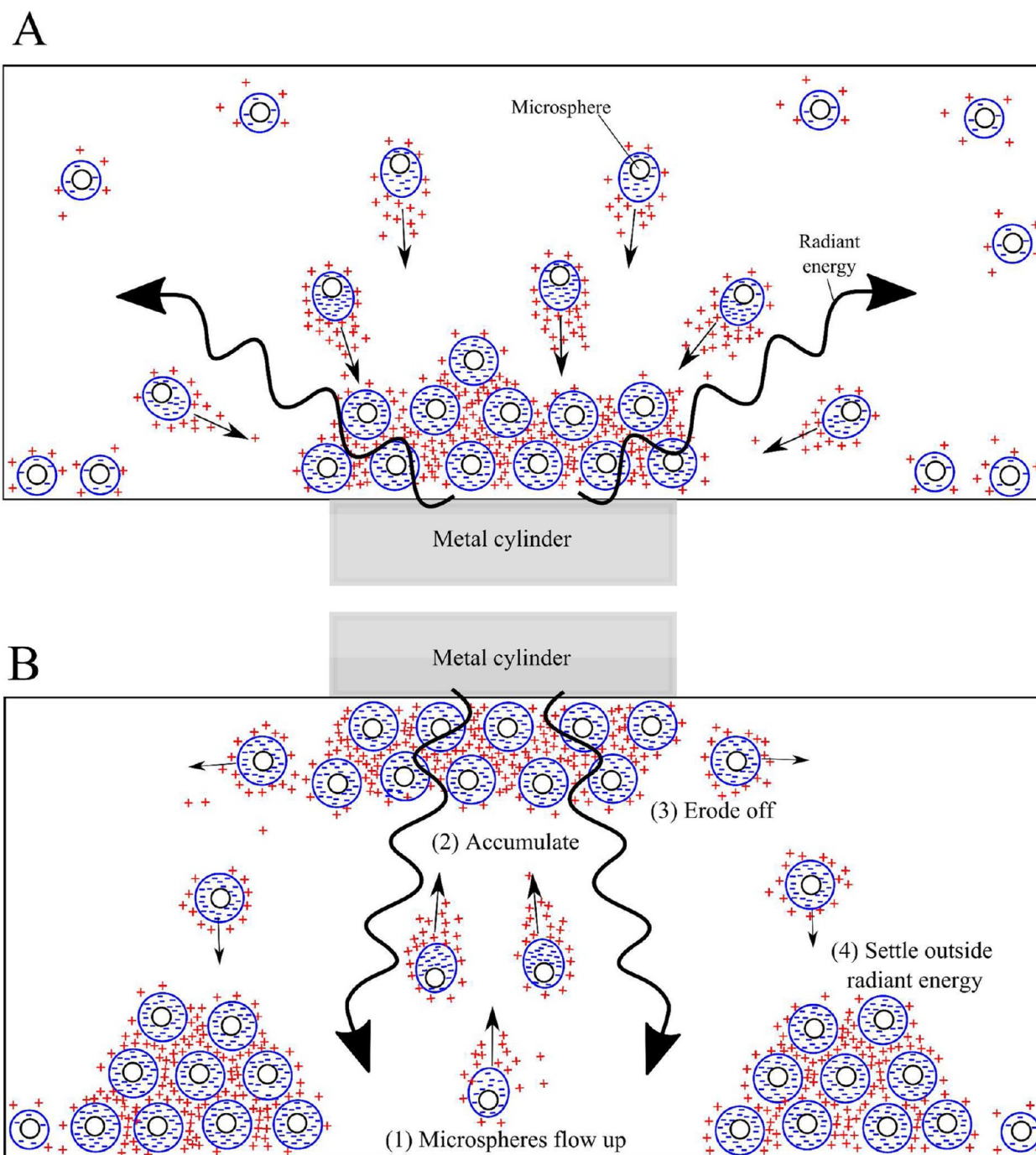


Figure 9. Diagrammatic sketch of proposed mechanism. (A) Metal emits radiant energy, which builds large EZs around microspheres. Those microspheres draw toward one another by the “like-likes-like” mechanism. Meanwhile, because incident light comes from one direction, those negatively charged EZs build asymmetrically, migrating in the direction of high positive charge. This direction is always toward the energy source, i.e., toward the metal. (B) Microspheres draw toward the metal on top, leaving a void beneath. As the concentration builds, the upward flow bends laterally, eroding some microspheres, which then sediment to the bottom of the chamber.

spheres? We were initially drawn to this series of experiments because we observed that magnets placed beneath the beaker caused concentrations similar to those observed here. When we substituted nonmagnetic metals, as shown in Figures 2 and 3, we observed similar results. This led us to conclude that magnetism was not responsible. A related possibility is that the carboxylate microspheres used may have had magnetic properties arising from iron compounds contained in added surfactants; however, the microspheres contained no surfactants, and several different types of microspheres gave similar

results. Also, glass, wood, and paper—all materials with no magnetic properties—produced some degree of accumulation.

Static Charge Hypothesis. Conceivably, some kind of static charge situated outside the chamber could play a role in the attraction. In theory, the metal piece beneath the Petri dish should not bear responsibility, for any charge on that metal will not conduct through the insulating Petri dish. The charge hypothesis was tested further by charging the subsurface metal to negative and/or positive 3 kV using a charge gun, and then measuring the surface charge on the other side with a surface-

charge meter. No significant charge was observed. Nor did we observe a noticeable difference of microsphere accumulation compared to the noncharged metal control. Additionally, charging the inner surface of the Petri dish had no noticeable effect on accumulation compared to the noncharged control; nor did submerging a charged piece of metal, or charging the metal piece beneath the Petri dish every hour for 10 h.

To further test the effects of external electric fields, the Petri dish containing the suspension was placed in the middle of a large high-voltage capacitor. To do this, two steel plates (10 cm × 20 cm × 2 mm) were placed on either side of the dish and connected to a power supply set at 20 kV. After a 24-h period, we could observe no obvious effect: the microspheres had settled uniformly. From these tests we conclude static electric fields have insignificant effect on microsphere accumulation.

Temperature-Gradient Hypothesis. Could the accumulation arise from a temperature difference between the aqueous region just above the metal and the rest of the suspension? In theory, a temperature difference could create a corresponding density difference, with warm water rising up from the bottom of the Petri dish directly above the metal disc, to the surface. This displaces the cooler bulk water, which eventually replaces the water directly above the metal disc. The result is a temperature-induced toroidal flow of water, centered above the metal disc. This flow could be gathering and concentrating microspheres settling to the bottom from the peripheral regions, resulting in microspheres accumulating in the middle.

We measured the temperatures in the region directly above the metal and in the bulk water, using a 1 mm thermocouple (Omega HH306A). At both locations temperatures were 20.1 °C (± 0.1 °C) before and after the 24-h period.

While the sensitivity limit of the thermocouple precludes detection of any temperature gradients smaller than 0.1 °C, it is unclear how any flow induced by any such minuscule density differences would force microspheres to accumulate in an almost perfect, clear-cut circle just above the metal cylinder. Nor does this hypothesis easily explain the void-ring formed when the metal was placed on top of the Petri dish.

Temperature can also impact surface tension. In theory, local temperature differences could induce surface tension gradients, which might induce unexpected flows, which could perhaps lead to unanticipated settling patterns. However, measured temperature gradients were small enough to deem this possibility unlikely.

Radiant-Energy Hypothesis. Another interpretational route follows from previous work on hydrophilic materials interfacing with water. Hydrophilic surfaces tend to order the interfacing water, sometimes out to considerable distances from those surfaces.⁹ These regions of ordered water have been called “exclusion zones” or EZs.⁸ EZs are interfacial water layers whose properties differ from those of bulk water. The interfacial water has been dubbed the “exclusion zone” because of its tendency to exclude solutes and particles. These micron-scale layers of water are more viscous than bulk water and generally bear negative charge.⁸ They build from radiant energy, most notably IR, but also UV and visible light.¹⁰

EZs build around hydrophilic particles in suspension such as those used here. Previous work has shown visually detectable EZs around microspheres with diameters ranging from several hundred micrometers down to near 10 μm ,¹⁰ implying that, although unresolvable by optical microscopy, EZs likely surround the smaller microspheres as well, such as the 1 μm microspheres used in this study.

Microspheres with negatively charged EZ layers are inherently attracted to each other because of the so-called “like-likes-like” phenomenon, first introduced by Feynman.¹¹ Positive ions naturally surround the negatively charged EZs. Those positive charges gather in between EZ-enveloped microspheres. Since opposite charges attract, the positive charges draw the negatively charged microspheres together. This concept has been experimentally confirmed by placing two macroscopic beads into water containing pH-sensitive dye. The dye confirmed the presence of opposite charges lying in between the beads,¹² drawing the beads toward one another and supporting Feynman’s contention that like-likes-like because of an intermediate of unlikes.¹¹

In the context of the experiments carried out here, radiant energy emitted from the metal should increase the EZs surrounding the microspheres. The EZ expansion increases both the negative charge and the intervening positive charge, enhancing the “like-likes-like” attraction. Experiments have indeed shown that increasing the incident light draws particles more closely together, even to the extent of forming an ordered structure.^{8,13} Additionally, as a control, when a solid piece of black cardstock was placed between the Petri dish and the metal piece to block any radiant energy emitted from the metal, effectively acting as an IR filter, no accumulation was observed.

Because the radiant energy is incident from a single direction, EZs will build asymmetrically; microsphere EZs will therefore develop asymmetric charge distributions (Figure 9A). Such asymmetric distributions have been observed.⁸ Positive charges will correspondingly gather in higher concentrations beyond the expanded EZs, drawing the microspheres toward the radiant energy source—in this case beneath the chamber, as observed.

The results obtained with the metal on top of the lid (Figure 7) may seem contradictory to the results with the metal beneath, because the microspheres vacate the region directly under the metal. However, Figure 9B shows that this result can be expected. Microspheres directly under the metal develop asymmetric charge distributions—in this instance pointing upward, toward the metal. The accompanying upward flow of water must deflect laterally as it reaches the upper surface, shearing past the growing microsphere cluster and eroding the cluster. The freed microspheres then settle outside of the range of radiant energy emitted from the metal, ultimately settling in high concentration in a ring peripheral to the upward flowing microspheres.

It is worth mentioning that ambient light reflecting off the metal disc could theoretically influence the observed accumulations. However, experiments carried out in light-tight, thermally insulated boxes gave similar results. Therefore, ambient light played a limited role in the present experiments.

A surprising and important result is that, once settled, microspheres still move in response to shifted metals (Figure 5). This indicates that the attractive force is able to overcome the adhesion forces keeping the microspheres settled. It emphasizes the remarkable strength of the attractive force driven by the radiant energy.

The radiant energy interpretation gains strength from the correlation between the strength of radiant emission (Figure 8) and the degree of concentration (Figure 4). Different materials radiate different wavelengths of infrared energy.¹⁴ Metals emit high IR intensities within the 7–14 μm range, while glass/wood emit low intensities (Figure 8). Although the exact distribution of emitted energy wavelengths could not be measured in these

experiments, we found reasonable correlation between experimentally determined IR intensity and accumulation. These IR intensities cannot be easily correlated with published emissivity values because the literature values depend strongly on metal surface conditions (e.g., oxidized versus unoxidized brass¹⁵); therefore, emissivity is often given in ranges. Along with correlation between IR intensities and accumulation, when incident visible light was used to increase IR emission, accumulation increased. Hence, these results lend support to the hypothesis that the observed concentrations arise from incident radiant energy.

Although IR wavelengths seem particularly relevant here, in the more general case, visible light also attracts microspheres.¹⁶ Hence, the role of radiant energy may be rather general, and not limited to the infrared region of the spectrum.

CONCLUSION

This work has revealed new, unanticipated features of aqueous colloidal suspensions. It appears that radiant energy emitted from ordinary materials, particularly metals, can attract suspended particles. When various materials are placed beneath the chamber containing the suspension, dramatic effects on the pattern of sedimentation can be produced. The central vehicle mediating the observed attraction and sedimentation appears to be interfacial (EZ) water, the latter highly responsive to the input of radiant energy.

Interfacial water plays a central role also in biological systems, where the mechanisms reported above may help to explain the positive health effects of sunlight^{17,18} or of the infrared energy generated by healing stones^{19,20} and artificial methods.²¹ At the very least, these findings throw new light on the mechanism of sedimentation, which may involve incident energy in unanticipated ways.

AUTHOR INFORMATION

Notes

The authors declare no competing financial interest.

ACKNOWLEDGMENTS

We acknowledge the advice of Drs. Hiromasa Ishiwatari, Kurt Kung, Rainer Stahlberg, and Wayne D. Kimura. We thank Jeff Magula for fabricating the metal discs and Rushi Panchal for his help editing the manuscript. This work was supported by NIH Transformative Grant T-R01 5R01GM093842.

REFERENCES

- (1) Philipse, A. Colloidal Sedimentation (and Filtration). *Curr. Opin. Colloid Interface Sci.* **1997**, *2* (2), 200–206.
- (2) Berg, J. *An Introduction to Interfaces & Colloids: The Bridge to Nanoscience*; World Scientific Publishing Company: Singapore, 2009.
- (3) Buscall, R. The Sedimentation of Concentrated Colloidal Suspensions. *Colloids Surf.* **1990**, *43*, 33–53.
- (4) Allouni, Z. E.; Cimpan, M. R.; Høl, P. J.; Skodvin, T.; Gjerdet, N. R. Agglomeration and Sedimentation of TiO₂ Nanoparticles in Cell Culture Medium. *Colloids Surf., B* **2009**, *68* (1), 83–87.
- (5) Giddings, J. C.; Karaiskakis, G.; Caldwell, K. D.; Myers, M. N. Colloid Characterization by Sedimentation Field-Flow Fractionation: I. Monodisperse Populations. *J. Colloid Interface Sci.* **1983**, *92* (1), 66–80.
- (6) Demeler, B.; Brookes, E. Monte Carlo Analysis of Sedimentation Experiments. *Colloid Polym. Sci.* **2008**, *286* (2), 129–137.
- (7) Moncho-Jordá, A.; Louis, A. A.; Padding, J. T. Effects of Interparticle Attractions on Colloidal Sedimentation. *Phys. Rev. Lett.* **2010**, *104* (6), 068301.

(8) Pollack, G. *The Fourth Phase of Water: Beyond Solid, Liquid, and Vapor*; Ebner and Sons Publishers: Seattle, WA, 2013.

(9) Jabs, H.; Rubik, B. Self-Organization at Aqueous Colloid-Membrane Interfaces and an Optical Method to Measure the Kinetics of Exclusion Zone Formation. *Entropy* **2014**, *16* (11), 5954–5975.

(10) Nhan, D. T.; Pollack, G. H. Effect of Particle Diameter on Exclusion-Zone Size. *Int. J. Nat. Ecodyn* **2011**, *6* (2), 139–144.

(11) Feynman, R.; Leighton, R.; Sands, M. *The Feynman Lectures on Physics*; Addison-Wesley: Reading, MA, 1964.

(12) Nagornyak, E.; Yoo, H.; Pollack, G. H. Mechanism of Attraction between like-Charged Particles in Aqueous Solution. *Soft Matter* **2009**, *5* (20), 3850–3857.

(13) Bunkin, N. F.; Ignatiev, P. S.; Kozlov, V. A.; Shkirin, A. V.; Zakharov, S. D.; Zinchenko, A. A. Study of the Phase States of Water close to Nafion Interface. *Water* **2013**, *4*, 129–154.

(14) Price, D. J. The Temperature Variation of the Emissivity of Metals in the near Infra-Red. *Proc. Phys. Soc.* **1947**, *59* (1), 131.

(15) Center for History and New Media. Zotero Quick Start Guide http://zotero.org/support/quick_start_guide.

(16) Velapagudi et al., Submitted.

(17) Egan, K. M.; Sosman, J. A.; Blot, W. J. Sunlight and Reduced Risk of Cancer: Is The Real Story Vitamin D? *JNCI J. Natl. Cancer Inst.* **2005**, *97* (3), 161–163.

(18) Mead, M. N. Benefits of Sunlight: A Bright Spot for Human Health. *Environ. Health Perspect.* **2008**, *116* (4), A160.

(19) Crichton, C. *Earth Medicine and Healing Stones: Practices for Health, Wealth & Longevity*; Konecky & Konecky: Old Saybrook, CT, 2006.

(20) Friedman, M. L. *Healing Spaces: Incorporating Gemstone and Chakra Healing into Architecture*, Ph.D. Thesis, University of Maryland, College Park, MD, 2012.

(21) Santana-Blank, L.; Rodríguez-Santana, E.; Reyes, H.; Santana-Rodríguez, J.; Santana-Rodríguez, K. Water-Light Interaction: A Novel Pathway for Multi Hallmark Therapy in Cancer. *Int. J. Cancer Ther. Oncol.* **2013**, *2* (1), 02012.